Photofragmentation of linear triatomics

O. Atabek, J. A. Beswick, and R. Lefebvre

Laboratoire de Photophysique Moléculaire, Orsay, France

S. Mukamel and J. Jortner

Department of Chemistry, Tel-Aviv University, Tel-Aviv, Israel
(Received 17 May 1976)

This paper is concerned with a complete quantum mechanical treatment for the photofragmentation of linear triatomic molecules, going beyond the Golden rule calculation and quasidiatomic approximation. Harmonic valence type potentials are assumed for the bound motions, while an exponential potential describes the unbound motion. An analytical expression for the final vibrational distribution is obtained. This explicitly incorporates the final states interactions which are responsible for the V–T energy transfer during the half-collision following the bond breaking. The two-dimensional Franck–Condon factors are evaluated using the Airy approximation, and a simplified statistical procedure to incorporate rotational distributions is presented. This treatment is applied to the photodissociation of ICN and HCN, and the effects of deuteration on linewidths are analyzed. A fit to the available experimental probability distribution leads to physically acceptable parameters for the repulsive potential.

I. INTRODUCTION

There has recently been considerable experimental[1–4] and theoretical[5–9] effort directed towards the elucidation of the dynamics of molecular photofragmentation of polyatomic species. The experiments provide the relative populations in the various internal states of the fragments (vibrational and rotational). The theory aims at relating this distribution to the excitation frequency and to the nature of the intervening electronic states of the parent molecule and of the fragments. From a methodological point of view, two problems must be considered:

(1) Data concerning the electronic states of the species have to be collected. This may come from an analysis of the electronic spectra,[10,11] as well as from semiempirical or *ab initio* calculations. This information serves as input in a formal theory of the fragmentation process.

(2) A variety of treatments of the fragmentation dynamics is possible, starting from simple Golden rule calculations[12] to a complete three-dimensional analysis. Along this chain, there is the collinear model, which should be acceptable in the case of triatomics having a linear geometry in all concerned electronic states.

The present paper applies the collinear model to the fragmentation of the triatomic cyanides XCN, with the assumption of rather simple potential energies. The treatment includes a proper handling of the normal modes problem,[9,13] thus relaxing the quasidiatomic approximation made in a previous paper.[7b] The intramolecular and interfragment[14–17] couplings are simultaneously included in order to assess the importance of the latter. Finally, an ad hoc formulation of the effect of rotational states is incorporated. The calculations are performed both in the relative coordinates and distorted wave approaches.

II. RELATIVE COORDINATES TREATMENT OF PHOTOFRAGMENTATION OF LINEAR TRIATOMICS

In the general quantum mechanical model,[7b] direct photodissociation and predissociation are described by a bound vibrational state of a Born–Oppenheimer (BO) electronic state $|s\rangle$ (which is the ground state for the direct photodissociation, and an excited state in the case of predissociation) coupled to a set of vibrational continua which correspond to another BO unbound electronic state $|d\rangle$. For a linear triatomic molecule (ABC) dissociating into A+BC fragments, these continua correspond to different vibrational states of the diatomic BC. The two electronic states $|s\rangle$ and $|d\rangle$ are coupled either by the electromagnetic field in the case of direct photodissociation or by intramolecular nonadiabatic coupling in predissociation. In this latter case, it is assumed that a light pulse has prepared the system in the $|s\rangle$ state.

The total wavefunctions for the two electronic states are

$$\begin{aligned} |\Psi_{s,v,v'}\rangle &= |\Theta^{(s)}\rangle |s,v,v'\rangle \,, \\ |\Psi_{d,n,\epsilon}\rangle &= |\Theta^{(d)}\rangle |d,n,\epsilon\rangle \,, \end{aligned} \tag{1}$$

where $|\Theta^{(s)}\rangle$ and $|\Theta^{(d)}\rangle$ are the electronic wavefunctions and $|s,v,v'\rangle$ and $|d,n,\epsilon\rangle$ the nuclear wavefunctions. Labels v and v' denote vibrational quantum numbers in the bound states, n corresponds to the vibrational quantum number of the diatomic fragment, and ϵ is the relative kinetic energy of the fragments.

In this section we shall consider the partitioning of the Hamiltonian utilizing a relative coordinate (RC) system.[16–18] An alternative approach, which involves expansion of the interfragment interaction in a power series of the intrafragments displacements, resulting in the first order distorted wave approximation, will be considered in Sec. IV. In the RC representation, the nuclear wavefunctions $|s,v,v'\rangle$ and $|d,n,\epsilon\rangle$ are the eigenfunctions of the Hamiltonian

$$H = -\frac{\hbar^2}{2}\left(\frac{1}{\mu_{AB}}\frac{\partial^2}{\partial R_{AB}^2} + \frac{1}{\mu_{BC}}\frac{\partial^2}{\partial R_{BC}^2} - \frac{2}{m_B}\frac{\partial^2}{\partial R_{AB}\partial R_{BC}}\right) + V^{(\beta)} \,, \tag{2}$$

where $\beta \equiv s$ or $\beta \equiv d$; R_{AB} and R_{BC} are the distances between atoms; μ_{AB} and μ_{BC} are reduced masses; and m_B is the mass of atom B. The motion of the center of mass of the entire system has been separated out. We

now invoke the assumption that in the two electronic states the potential $V^{(\beta)}$ can be expressed as a sum of two potentials between adjacent particles. This is a very common approximation in the treatment of energy transfer between vibration and translation in the collinear model. For the linear molecule (ABC) this implies that

$$V^{(\beta)} = V_{AB}^{(\beta)}(R_{AB}) + V_{BC}^{(\beta)}(R_{BC}) \qquad \beta = s, d \ . \tag{3}$$

For the bound state $|s\rangle$ the two potentials are supposed to be harmonic,

$$V_{AB}^{(s)}(R_{AB}) = 1/2\mu_{AB}\omega_{AB}^{(s)2}(R_{AB} - \bar{R}_{AB}^{(s)})^2 \ , \tag{4}$$

$$V_{BC}^{(s)}(R_{BC}) = 1/2\mu_{BC}\omega_{BC}^{(s)2}(R_{BC} - \bar{R}_{BC}^{(s)})^2 \ , \tag{5}$$

where the force constants of the AB and BC bonds are $k_{AB}^{(s)} \equiv \mu_{AB}\omega_{AB}^{(s)2}$ and $k_{BC}^{(s)} \equiv \mu_{BC}\omega_{BC}^{(s)2}$, respectively, being expressed in terms of the bond frequencies $\omega_{AB}^{(s)}$ and $\omega_{BC}^{(s)}$.

For the dissociative state $|d\rangle$, $V_{AB}^{(d)}$ is taken as a pure exponential repulsive potential, whereas $V_{BC}^{(d)}$ is still assumed to be harmonic:

$$V_{AB}^{(d)}(R_{AB}) = U e^{-aR_{AB}} \ , \tag{6}$$

$$V_{BC}^{(d)}(R_{BC}) = 1/2\mu_{BC}\omega_{BC}^{(d)2}(R_{BC} - \bar{R}_{BC}^{(d)})^2 \ . \tag{7}$$

Here $\omega_{BC}^{(d)}$ corresponds to the frequency of the diatomic fragment.

Now making use of the dimensionless coordinates

$$y = (\mu_{BC}\omega_{BC}^{(d)}/\hbar)^{1/2}(R_{BC} - \bar{R}_{BC}^{(d)}) \ , \tag{8}$$

$$z = (\mu_{BC}\omega_{BC}^{(d)}/\hbar)^{1/2}[(m_B + m_C)/m_C]R_{AB} \tag{9}$$

and the following definitions,

$$A = U/\hbar\omega_{BC}^{(d)} \ , \tag{10}$$

$$\alpha = a[m_C/(m_B + m_C)](\mu_{BC}\omega_{BC}^{(d)}/\hbar)^{-1/2} \ , \tag{11}$$

$$\bar{m} = \mu_{AB}\mu_{BC}/m_B^2 \ , \tag{12}$$

the nuclear Hamiltonian for the dissociative state takes the form (energies are measured in units of $\hbar\omega_{BC}^{(d)}$)

$$H^{(d)} = -(1/2\bar{m})\frac{\partial^2}{\partial z^2} - 1/2\frac{\partial^2}{\partial y^2} + 1/2y^2 + A e^{-\alpha z} + \frac{\partial^2}{\partial y \partial z} \ , \tag{13}$$

while for the bound state $|s\rangle$ the nuclear Hamiltonian is

$$H^{(s)} = -(1/2\bar{m})\frac{\partial^2}{\partial z^2} - 1/2\frac{\partial^2}{\partial y^2} + 1/2\Omega_{BC}^2(y - \bar{y})^2 + 1/2\bar{m}\Omega_{AB}^2(z - \bar{z})^2 + \partial^2/\partial y \partial z \ , \tag{14}$$

where

$$\bar{y} = (\mu_{BC}\omega_{BC}^{(d)}/\hbar)^{1/2}(\bar{R}_{BC}^{(s)} - \bar{R}_{BC}^{(d)}) \ ,$$

$$\bar{z} = (\mu_{BC}\omega_{BC}^{(d)}/\hbar)^{1/2}[(m_B + m_C)/m_C]\bar{R}_{AB}^{(s)} \ , \tag{15}$$

$$\Omega_{BC} = \omega_{BC}^{(s)}/\omega_{BC}^{(d)}, \qquad \Omega_{AB} = \omega_{AB}^{(s)}/\omega_{BC}^{(d)} \ .$$

Now using the Rosen partitioning,[18] we keep that part of $H^{(d)}$ separable in y and z. The kinetic energy cross term $\partial^2/\partial y \partial z$ is incorporated at a later stage. This results in zero order eigenfunctions for the dissociative channels having the form

$$|d, n, \epsilon\rangle = |\chi_n^{(d)}(y)\rangle\,|\phi_\epsilon(z)\rangle \ , \tag{16}$$

where $|\chi_n^{(d)}(y)\rangle$ is the harmonic oscillator wavefunction with energy $(n + 1/2)$, and $|\phi_\epsilon(z)\rangle$ is the solution of

$$\left[-\frac{1}{2\bar{m}}\frac{\partial^2}{\partial z^2} + A e^{-\alpha z} - \epsilon\right]|\phi_\epsilon(z)\rangle = 0 \ . \tag{17}$$

This wavefunction is

$$|\phi_\epsilon(z)\rangle = \frac{2}{\pi}\left[\frac{\bar{m}}{\alpha}\sinh\left(\frac{2\pi\bar{k}}{\alpha}\right)\right]^{1/2} K_\nu(\theta) \ , \tag{18}$$

with

$$\bar{k} = (2\bar{m}\epsilon)^{1/2} \ ,$$

$$\nu = (2i\bar{k}/\alpha) \ , \tag{19}$$

$$\theta = (2/\alpha)(2A\bar{m}\, e^{-\alpha z})^{1/2} \ ,$$

$K_\nu(\theta)$ is the modified Bessel function.[21] The wavefunctions (16) with $|\phi_\epsilon(z)\rangle$ given by (18) are energy normalized,

$$\langle d, n', \epsilon' | d, n, \epsilon\rangle = \delta_{nn'}\delta(\epsilon - \epsilon') \ , \tag{20}$$

and the asymptotic form of $|d, n, \epsilon\rangle$ for $z \to +\infty$ is

$$|d, n, \epsilon\rangle_{z\to+\infty} \cong |\chi_n^{(d)}(\nu)\rangle\left(\frac{2\bar{m}}{\pi\bar{k}}\right)^{1/2}\cos(\bar{k}z - \theta) \ , \tag{21}$$

with

$$\theta = (\bar{k}/\alpha)\log(2A\bar{m}/\alpha^2) - \arg\Gamma(\nu) \ . \tag{22}$$

For the bound state $|s\rangle$ it is possible to construct exact eigenfunctions of (14) by using normal coordinates, in terms of which the nuclear Hamiltonian takes the form

$$H^{(s)} = \omega_1\left[-1/2\frac{\partial^2}{\partial q_1^2} + 1/2q_1^2\right] + \omega_2\left[-1/2\frac{\partial^2}{\partial q_2^2} + 1/2q_2^2\right], \tag{23}$$

where ω_1 and ω_2 are the molecular frequencies corresponding to the normal modes q_1 and q_2 (note that both frequencies are normalized by $\omega_{BC}^{(d)}$).

The total vibronic wavefunction $|s, v, v'\rangle$ [see Eq. (1)] assumes the form

$$|s, v, v'\rangle = |\chi_v^{(s)}(q_1)\rangle\,|\chi_{v'}^{(s)}(q_2)\rangle \ , \tag{24}$$

where χ_v and $\chi_{v'}$ are harmonic oscillator wavefunctions with energies $\omega_1(v + 1/2)$ and $\omega_2(v' + 1/2)$, respectively.

Band and Freed[9] have pointed out that a proper evaluation of discrete–continuum coupling terms requires a transformation between the normal coordinates (q_1, q_2) of the bound state and those specifying the dissociative state, and attempted to provide such a transformation[9d] in terms of the distorted wave representation. In what follows we shall present the appropriate coordinate transformation in the relative coordinate representation, while the distorted wave representation will be considered in Sec. IV. The coordinates q_1 and q_2, Eq. (23), are related to relative coordinates y and z, Eqs. (8), (9), and (15), by the linear transformation

$$\begin{pmatrix} q_1 \\ q_2 \end{pmatrix} = \begin{pmatrix} C_{11} & C_{12} \\ C_{21} & C_{22} \end{pmatrix}\begin{pmatrix} z - \bar{z} \\ y - \bar{y} \end{pmatrix} \ , \tag{25}$$

with

$$C_{11} = \frac{\bar{m}^{1/2}\Omega_{AB}\omega_1^{-1/2}}{\sqrt{2(\omega_2^2 - \omega_1^2)}}\left[(\Omega_{BC}^2 - \Omega_{AB}^2) + (\omega_2^2 - \omega_1^2)\right]^{1/2} \ ,$$

$$C_{12} = \frac{\Omega_{BC}\omega_1^{-1/2}}{\sqrt{2(\omega_2^2 - \omega_1^2)}}\left[-(\Omega_{BC}^2 - \Omega_{AB}^2) + (\omega_2^2 - \omega_1^2)\right]^{1/2} \ ,$$

$$C_{21} = -\frac{\bar{m}^{1/2}\Omega_{AB}\omega_2^{-1/2}}{\Omega_{BC}\omega_1^{-1/2}} C_{12} ,$$

$$C_{22} = \frac{\Omega_{BC}\omega_2^{-1/2}}{\bar{m}^{1/2}\Omega_{AB}\omega_1^{-1/2}} C_{11} . \quad (26)$$

The transformation matrix C, Eqs. (25) and (26), may be readily evaluated using the experimental data for the atomic masses, the spectroscopic molecular frequencies ω_1 and ω_2 of the ABC molecule, and the frequency $\omega_{BC}^{(d)}$ of the BC radical. The parameters Ω_{AB} and Ω_{BC}, Eq. (15), are expressed in the following manner:

$$\Omega_{AB}^2 + \Omega_{BC}^2 = \omega_1^2 + \omega_2^2 ,$$
$$(4\bar{m} - 2)\Omega_{BC}^2\Omega_{AB}^2 = (\omega_2^2 - \omega_1^2)^2 - \omega_1^2 - \omega_2^2 , \quad (27)$$

resulting in the simple relations

$$\omega_1 = \left(\frac{\Omega_{AB}^2 + \Omega_{BC}^2}{2} - \frac{\Delta}{2}\right)^{1/2} ,$$
$$\omega_2 = \left(\frac{\Omega_{AB}^2 + \Omega_{BC}^2}{2} + \frac{\Delta}{2}\right)^{1/2} , \quad (27')$$
$$\Delta = [(\Omega_{BC}^2 - \Omega_{AB}^2)^2 + 4\bar{m}\Omega_{BC}^2\Omega_{AB}^2]^{1/2} .$$

III. INTRAFRAGMENT AND INTERFRAGMENT COUPLING

The photofragmentation process can be conceptualized in terms of coupling between the BO zero order states $|\Psi_{s,v,v'}\rangle$ and $|\Psi_{d,n,\epsilon}\rangle$ [Eqs. (1), (16), and (24)], which are characterized by the energies

$$E_{s,v,v'} = E_s^0 + (v + \tfrac{1}{2})\omega_1 + (v' + \tfrac{1}{2})\omega_2 ,$$
$$E_{d,n,\epsilon} = E_d^0 + (n + \tfrac{1}{2}) + \epsilon , \quad (28)$$

where E_s^0 and E_d^0 correspond to the electronic origins of the two states. In the case of predissociation, the interstate coupling involves just nonadiabatic coupling terms H_v, while for the case of direct photodissociation the BO representation for pure spin states is adequate and the interstate coupling is induced by the radiative interaction H_{int}. In addition, the zero order nuclear wavefunctions for the dissociative state, Eq. (16), are coupled by the intrastate coupling term $\partial^2/\partial y \partial z$. The total Hamiltonian for the system can be recast in the form

$$H = H_0 + V , \quad (29)$$

where the zero order Hamiltonian is

$$H_0 = \sum_n \int dE_{d,n,\epsilon} |\Psi_{d,n,\epsilon}\rangle E_{d,n,\epsilon} \langle\Psi_{d,n,\epsilon}|$$
$$+ \sum_v \sum_{v'} |\Psi_{s,v,v'}\rangle E_{s,v,v'} \langle\Psi_{s,v,v'}| , \quad (29')$$

and the perturbation terms are given by

$$V = \sum_v \sum_{v'} \sum_n \int dE_{dn\epsilon} (|\Psi_{svv'}\rangle V_{svv',dn\epsilon} \langle\Psi_{dn\epsilon}| + \text{C.C.})$$
$$+ \sum_n \sum_{n'} \iint dE_{dn\epsilon} dE_{dn'\epsilon'} |\Psi_{dn\epsilon}\rangle V_{dn\epsilon,dn'\epsilon'} \langle\Psi_{dn'\epsilon'}| , \quad (29'')$$

involving both interstate (bound–continuum) and intrastate (continuum–continuum) coupling. The interstate coupling is

$$V_{svv',dn\epsilon} = \langle\Psi_{svv'}|X|\Psi_{dn\epsilon}\rangle , \quad (30)$$

being expressed in terms of the perturbation $X = H_v$ for predissociation and $X \equiv H_{int}$ for direct photodissociation. The interstate coupling in the dissociative state is given by

$$V_{dn\epsilon,dn'\epsilon'} = \langle d, n, \epsilon | \partial^2/\partial y \partial z | d, n', \epsilon' \rangle . \quad (31)$$

We now proceed to the evaluation of the two types of coupling terms, Eqs. (30) and (31), which enter in our model.

A. Discrete-continuum coupling

Invoking the Condon approximation, the interstate coupling Eq. (30) reduces to

$$V_{svv',dn\epsilon} = \langle\Theta^{(s)}|X|\Theta^{(d)}\rangle \langle s, v, v' | d, n, \epsilon\rangle , \quad (32)$$

where the wavefunctions are defined by Eq. (1). We thus have discrete–continuum couplings which are proportional to the generalized Franck–Condon factors: $\langle s, v, v' | d, n, \epsilon\rangle$. Using Eqs. (16) and (24), they can be written in the form

$$\langle s, v, v' | d, n, \epsilon\rangle = (\det)^{1/2} \int_{-\infty}^{+\infty} dy \int_{-\infty}^{+\infty} dz\, \chi_n^{(d)}(y)\phi_\epsilon(z)\chi_v^{(s)}(q_1)\chi_{v'}^{(s)}(q_2) , \quad (33)$$

where

$$\chi^{(d)}(y)$$

and

$$\chi^{(s)}(q_i) \quad (i = 1, 2)$$

are harmonic oscillator wavefunctions, and $\phi_\epsilon(z)$ is defined by Eq. (18). $\det = \bar{m}^{1/2}\Omega_{AB}\Omega_{BC}/(\omega_1\omega_2)^{1/2}$ denotes the determinant of the coordinates transformation (25). The two-dimensional integral in Eq. (33) can be transformed to a sum of one-dimensional integrals by applying the method of Band and Freed.[9] This procedure, outlined in Appendix A, results in

$$\langle s, v, v' | d, n, \epsilon\rangle = (\det)^{1/2}\pi^{-1/4}(1 + C_{12}^2 + C_{22}^2)^{-1/2} 2^{-(v+v'+n-1)/2}(v!\,v'!\,n!)^{-1/2}$$
$$\times \sum_{r_1=0}^{v} \sum_{r_2=0}^{v'} \sum_{r_3=0}^{n} d_1^{v-r_1} d_2^{v'-r_2} d_3^{n-r_3} \binom{v}{r_1}\binom{v'}{r_2}\binom{n}{r_3} \mathcal{F}(v + v' + n - r_1 - r_2 - r_3) T(r_1, r_2, r_3) . \quad (34)$$

The coefficients d_i are given by

$$d_i = d\tilde{z}/dt_i , \quad (35)$$

where $\tilde{z}$ is defined by Eq. (A5), and the functions $\mathcal{F}$ and T are defined by

$$\mathcal{F}(N) = \int_{-\infty}^{\infty} dz\, \phi_\epsilon(z) \frac{d^N}{d\tilde{z}^N} e^{-1/2\tilde{\omega}(z-\tilde{z})^2} \Big|_{t_1,t_2,t_3=0} \quad (36a)$$

and

$$T(r_1, r_2, r_3) = \left(\frac{\partial}{\partial t_1}\right)^{r_1}\left(\frac{\partial}{\partial t_2}\right)^{r_2}\left(\frac{\partial}{\partial t_3}\right)^{r_3} \times \exp[f(t_1, t_2, t_3)]\Big|_{t_1, t_2, t_3=0} . \quad (36b)$$

$f(t_1, t_2, t_3)$ is defined by Eq. (A6). Evaluation of the integral Eq. (36a) cannot be performed analytically for the modified Bessel function $\phi_\epsilon(z)$, and a numerical integration method has to be applied. Band and Freed[9] linearized the repulsive potential around the classical turning point, and this approximation results in an analytical expression of Eq. (34). In our case we then have

$$\mathcal{F}(0) = \sqrt{\frac{4\pi\bar{m}}{\tilde{\omega}\gamma}}\exp[\gamma^6/12\tilde{\omega}^3 + \gamma^3(z_t - \tilde{z})/2\tilde{\omega})] \times \mathrm{Ai}\left[\frac{\gamma^4}{4\tilde{\omega}^2} + \gamma(z_t - \tilde{z})\right]\Big|_{t_1, t_2, t_3=0} , \quad (37)$$

with

$$\gamma = (\alpha\bar{k}^2)^{1/3}, \qquad Z_t = \ln\left[\left(\frac{2\bar{m}A}{\bar{k}^2}\right)^{1/\alpha}\right] . \quad (38)$$

The higher order functions $\mathcal{F}(N)$ are easily obtained by taking the nth order derivative of Eq. (37) with respect to $\tilde{z}$ and using the recursion relations[19] for the Airy function,

$$\frac{d^N \mathrm{Ai}(z)}{dz^N} = \frac{z d^{N-2}\mathrm{Ai}(z)}{dz^{N-2}} + (N-2)\frac{d^{N-3}\mathrm{Ai}(z)}{dz^{N-3}} . \quad (39)$$

Explicit expressions for a special case where $v = v' = 0$ in the bound state are presented in Appendix B. The $T(r_1, r_2, r_3)$ factor may be also evaluated using recurrence relations.[9]

The interest in this linear approximation is that it can be generalized to polyatomics involving more than three atoms. We have accordingly performed numerical integrations of Eq. (36a) to test the validity of this approximation. For the parameter α of the exponential repulsive potential corresponding to real life situations (i.e., α in the range of 0.1 to 0.3), the discrepancies between the results of the linear approximation and those obtained from numerical integration of Eqs. (34)–(36) are very small if the kinetic energy exceeds one quantum of the diatomic vibration.

B. Continuum-continuum couplings

Turning back now to the dissociative state, the interfragment coupling terms, Eq. (31), are

$$V_{dn\epsilon, dn'\epsilon'} = \langle\chi_n^{(d)}|\frac{\partial}{\partial y}|\chi_{n'}^{(d)}\rangle\langle\phi_\epsilon|\frac{\partial}{\partial z}|\phi_{\epsilon'}\rangle . \quad (40)$$

These coupling terms have already been discussed in detail in previous studies of V–T transfer.[16,17] The main features are as follows:

(a) Intracontinuum coupling prevails only between adjacent continua, i.e., for $n' = n \pm 1$.

(b) For $\epsilon \sim \epsilon'$ Eq. (40) behaves like a principal part distribution producing "persistent effects" and leading to a redefinition of the asymptotic states and energy. In first approximation one has only to consider energy shifts; this ultimately leads to the replacement of $\bar{m}$ by $m = (m_A m_C/m_B M)$ in the expression for $\bar{k}$, Eq. (19).

(c) These matrix elements can finally be expressed as

$$V_{d,n,\epsilon;d,n+1,\epsilon'} = \frac{\bar{m}}{\sqrt{2\alpha}}(n+1)^{1/2}\sinh^{1/2}(2\pi k/\alpha) \times \sinh^{1/2}(2\pi k'/\alpha)\,\mathrm{csch}[(\pi/\alpha)(k+k')] \times \mathrm{csch}[(\pi/\alpha)(k-k')] , \quad (41)$$

with

$$k = (2m\epsilon)^{1/2}, \qquad k' = (2m\epsilon')^{1/2} . \quad (42)$$

IV. PHOTOFRAGMENTATION IN THE DISTORTED WAVE BASIS

In the preceding sections we have used relative coordinates and the Rosen partitioning of the Hamiltonian[18] to represent the zero-order basis in the repulsive state $|d\rangle$. In the distorted wave approximation,[20] the Hamiltonian for the repulsive state is written in terms of the distance between atoms B and C (R_{BC}) and the distance between atom A and the center of mass of the BC molecule

$$R_{A(BC)} = R_{AB} + \frac{m_C}{m_B + m_C} R_{BC} . \quad (43)$$

As in Sec. II, it is convenient to define two reduced coordinates[21]

$$y = \left(\frac{\mu_{BC}\omega_{BC}^{(d)}}{\hbar}\right)^{1/2}(R_{BC} - \bar{R}_{BC}^{(d)}) ,$$
$$x = \left(\frac{\mu_{BC}\omega_{BC}^{(d)}}{\hbar}\right)^{1/2}(R_{A(BC)} - \bar{R}_{BC}^{(d)})\left(\frac{m_B + m_C}{m_C}\right) , \quad (44)$$

in terms of which the Hamiltonian for the repulsive state is

$$H^{(d)} = -\frac{1}{2m}\frac{\partial^2}{\partial x^2} - \frac{1}{2}\frac{\partial^2}{\partial y^2} + \tfrac{1}{2}y^2 + A\,e^{-\alpha(x-y)} , \quad (45)$$

with

$$m = m_A m_C/m_B M . \quad (46)$$

We see immediately, by comparing these equations with those given in Sec. II, that coordinates y and x are related to y and z, Eqs. (8) and (9), by the transformation

$$y = y, \qquad z = x - y , \quad (47a)$$

and that

$$\bar{m} = m/(1+m) . \quad (47b)$$

Thus the transformation between the normal coordinates (q_1, q_2) of the bound state, Eq. (25), and the coordinates x and y would be

$$\begin{pmatrix} q_1 \\ q_2 \end{pmatrix} = \begin{pmatrix} C'_{11} & C'_{12} \\ C'_{21} & C'_{22} \end{pmatrix}\begin{pmatrix} x - \bar{x} \\ y - \bar{y} \end{pmatrix}, \quad (48)$$

with

$$\bar{x} = \bar{z} + \bar{y} , \quad (49)$$

and $\bar{y}$ given by Eq. (15). The coordinate transformation, Eq. (48), appropriate for the distorted wave ba-

sis, was originally given by Band and Freed.[9] This transformation matrix C', Eq. (48), is related to the transformation matrix C, Eq. (25), in the relative coordinate representation via

$$C'_{11}=C_{11},\quad C'_{12}=C_{12}-C_{11},\quad C'_{21}=C_{21},\quad C'_{22}=C_{22}-C_{21},$$

where $\bar{z}$, $\bar{y}$, $\{C_{ij}\}$ have been defined in Sec. II.

For the zero-order nuclear wavefunction in the distorted wave approximation, we write

$$|d,n,\epsilon\rangle=|\chi_n^{(d)}(y)\rangle\,|\phi_{\epsilon,n}(x)\rangle\,, \tag{50}$$

where $|\chi_n^{(d)}(y)\rangle$ is the harmonic oscillator wavefunction with energy $(n+1/2)$, and $|\phi_{\epsilon,n}(x)\rangle$ is the solution of

$$\left[-\frac{1}{2m}\frac{\partial^2}{\partial x^2}+A_n e^{-\alpha x}-\epsilon\right]|\phi_{\epsilon,n}(x)\rangle=0\,, \tag{51}$$

with

$$A_n=A\langle\chi_n^{(d)}\,|\,e^{\alpha y}\,|\,\chi_n^{(d)}\rangle_y\,. \tag{52}$$

It should be noted that $|\phi_{\epsilon,n}(x)\rangle$ has the same form as in relative coordinates [Eq. (17)] with m replacing $\bar{m}$ and A_n, Eq. (52), replacing A. The first-order distorted wave approximation (FODWA) is based on the linearization of the interfragment potential with respect to y (i.e., setting $e^{\alpha y}\simeq 1+\alpha y$). In this case, $A_n=A$ and the intercontinuum coupling assumes the form

$$\begin{aligned}V_{dn'\epsilon',dn\epsilon}&\equiv\langle d,n',\epsilon'\,|\,(H^{(d)}-E)\,|\,d,n,\epsilon\rangle\\&=A\langle\phi_{\epsilon',n'}\,|\,e^{-\alpha x}\,|\,\phi_{\epsilon,n}\rangle_x\langle\chi_{n'}\,|\,e^{\alpha y}\,|\,\chi_n\rangle_y\,.\end{aligned} \tag{53}$$

In relative coordinates and in the FODWA, these intercontinuum couplings have the same form; the only difference is that in the relative coordinates approximation m is replaced by $\bar{m}$.[16,17] For the discrete–continuum interstate couplings, we have the following result for the overlap integrals:

$$\begin{aligned}&\langle s,v,v'\,|\,d,n,\epsilon\rangle\\&=(\det)^{1/2}\int_{-\infty}^{\infty}\int_{-\infty}^{\infty}dxdy\chi_v^{(s)}(q_1)\chi_{v'}^{(s)}(q_2)\chi_n^{(d)}(y)\phi_{\epsilon,n}(x)\,,\end{aligned} \tag{54}$$

and again, all the calculations presented in Sec. III can be transposed here, by merely replacing $\bar{m}$ by m, $\{C_{ij}\}$ by $\{C'_{ij}\}$, A by A_n, and $\bar{z}$ by $\bar{x}$.

V. DECAY SCHEME FOR PHOTOFRAGMENTATION AND FINAL VIBRATIONAL DISTRIBUTION

The decay scheme for photofragmentation[7] involves an initial discrete state $|s,v,v'\rangle$ coupled to an infinite number of interacting continua $\{|d,n,\epsilon\rangle\}$ $(n=0,1,\ldots)$. For simplicity, we are going to denote the zero order states by $|s\rangle\equiv|s,v,v'\rangle$; $|n,\epsilon\rangle\equiv|d,n,\epsilon\rangle$ and the couplings by $V_{s,n\epsilon}$ for the discrete–continuum interaction and by $V_{n\epsilon,n'\epsilon'}$ for the continuum–continuum interaction. The probability to be in the nth continuum at time t, if at time $t=0$ the system was in the discrete state $|s\rangle$, is[22]

$$p_n(t)=\frac{1}{4\pi^2}\int dE_{n\epsilon}\left|\int_{-\infty}^{+\infty}dE G^{+}_{n\epsilon,s}(E)\,e^{-iEt}\right|^2\,, \tag{55}$$

where $G^{+}_{n\epsilon,s}$ is the matrix element of the Green's function $G^{+}(E)=(E^{+}-H+i\eta)^{-1}$, $\eta\to 0^{+}$, $E_{n\epsilon}$ is the total (zero-order) energy of the state $|n\epsilon\rangle$ [in our case it will be $E_{n\epsilon}=(n+1/2)+\epsilon$]. The final probability distribution of the fragments among the vibrational channels is

$$P_n=p_n(\infty)\,. \tag{56}$$

The evaluation of the matrix elements of the Green's function in Eq. (55) can be accomplished[7] by the application of the projection operators method.[23] Let us define the projection operators

$$\hat{P}=|s\rangle\langle s|$$

and

$$\hat{Q}=1-\hat{P}=\sum_n\int dE_{n\epsilon}\,|n\epsilon\rangle\langle n\epsilon|\,. \tag{57}$$

The calculation of $G_{n\epsilon,s}(E)$ in Eq. (45) requires the projection $\hat{Q}G\hat{P}$, which has the form[23]

$$\hat{Q}G\hat{P}=(E-\hat{Q}H_0\hat{Q})^{-1}\hat{Q}\hat{R}\hat{P}(E-H_0-\hat{P}\hat{R}\hat{P})^{-1}\hat{P}\,, \tag{58}$$

where we have used the dissection $H=H_0+V$ of the Hamiltonian according to Eq. (29). The level-shift operator $\hat{R}$ is

$$\hat{R}=V+V(E-\hat{Q}H\hat{Q})^{-1}\hat{Q}V\,, \tag{59}$$

which can be separated into its Hermitian and anti-Hermitian parts,

$$\hat{R}=\hat{\Delta}-\tfrac{1}{2}i\hat{\Gamma}\,, \tag{60}$$

$$\hat{\Delta}=V+V[\mathrm{PP}(E-\hat{Q}H\hat{Q})^{-1}]\hat{Q}V\,, \tag{60'}$$

$$\hat{\Gamma}=2\pi V\delta(E-\hat{Q}H\hat{Q})V\,, \tag{60''}$$

where PP in Eq. (60′) denotes the principal part of the integral. Making use of Eqs. (58)–(60), we get for the relevant matrix elements

$$\langle n\epsilon\,|\,\hat{Q}G\hat{P}\,|\,s\rangle=\frac{\langle n\epsilon|\,\hat{Q}\hat{R}\hat{P}|\,s\rangle}{(E-E_{n\epsilon}+i\eta)(E-E_s-\Delta_s+\frac{1}{2}i\Gamma_s)}\,, \tag{61}$$

where

$$\begin{aligned}\Delta_s&=\langle s\,|\,\hat{\Delta}\,|\,s\rangle\,,\\ \Gamma_s&=\langle s\,|\,\hat{\Gamma}\,|\,s\rangle\,.\end{aligned} \tag{62}$$

We may now perform the integration in Eq. (55) by invoking the usual assumption regarding the weak energy dependence of the matrix element of R in Eq. (61).[22] The probability distribution is[7]

$$p_n(t)=\frac{2\pi}{\Gamma_s}\,|\langle n\epsilon\,|\,\hat{Q}\hat{R}\hat{P}\,|\,s\rangle|^2[1-\exp(-\Gamma_s t)] \tag{63}$$

and

$$P_n=\frac{2\pi}{\Gamma_s}\,|\langle n\epsilon\,|\,\hat{Q}\hat{R}\hat{P}\,|\,s\rangle|^2\,. \tag{64}$$

We are now able to separate formally the contribution of the Franck–Condon interstate couplings terms $\hat{Q}V\hat{P}$ and the intercontinuum coupling $\hat{Q}V\hat{Q}$. Defining the wave operator $\hat{F}$ for (half) collision on the dissociative potential surface

$$\hat{Q}\hat{F}\hat{Q}=\hat{Q}+\hat{Q}V\hat{Q}(E-\hat{Q}H\hat{Q})^{-1}\,, \tag{65}$$

we obtain

$$\hat{Q}\hat{R}\hat{P}=\hat{Q}\hat{F}\hat{Q}V\hat{P}\,. \tag{66}$$

Equations (64) and (66) constitute the formal solution to

the photofragmentation problem where the contributions of interfragment coupling $\hat{Q}\hat{F}\hat{Q}$ and intrafragment coupling $\hat{Q}V\hat{P}$ have been separated out.[7b] To obtain an explicit result for P_n we take only on-the-energy-shell contributions, whereupon Eq. (64) for the vibrational distribution probabilities takes the form[7,17]

$$P_n = \frac{|\sum_{n'} F(n,n')V_{n's}|^2}{R_e \sum_n \sum_{n'} V_{sn'} F(n,n') V_{n's}} , \tag{67}$$

where

$$F(n,n') = \langle n\epsilon | \hat{Q}\hat{F}\hat{Q} | n'\epsilon \rangle . \tag{68}$$

It can be also easily shown[7] that the total photofragmentation probability which can be expressed in terms of Eqs. (65) and (60'') takes the form

$$\Gamma_s = 2\pi |\langle \Theta^{(s)} | X | \Theta^{(d)} \rangle|^2 \gamma_s ,$$
$$\gamma_s = R_e \sum_n \sum_{n'} V_{sn} F(n,n') V_{n's} , \tag{69}$$

where the electronic matrix element $\langle \Theta^{(s)} | X | \Theta^{(d)} \rangle$ appears in Eq. (32). In the case of predissociation, Γ_s corresponds to the predissociation probability from an "initially prepared" bound electronically excited state, while the direct photodissociation Γ_s denotes (apart from irrelevant proportionality constants) the photodissociation cross section accessible by optical excitation at the energy E.

Equations (67)–(69) incorporate the relevant information concerning photofragmentation dynamics in terms of the (half) collision matrix $\hat{F}$. In our previous work,[7,17] we have advanced a first order K matrix approximation for the $\hat{F}$ matrix (defined in the $\hat{Q}$ subspace), which assumes the simple form

$$\hat{Q}\hat{F}\hat{Q} = (1 + i\pi\hat{Q}V\hat{Q})^{-1} . \tag{70}$$

In this model the $\hat{F}$ matrix can be expressed in an analytical form,[17]

$$F(n,n') = \frac{Q_\alpha \bar{Q}_\beta}{Q_N} \prod_{j=\alpha}^{\beta-1} (-i\pi V_{j,j+1}) , \tag{71}$$

with $\alpha = \min(n,n')$, $\beta = \max(n,n')$; Q_α and Q_β are polynomials determined by the recurrence relations

$$Q_0 = Q_1 = 1 ,$$
$$Q_{j+1} = Q_j + \pi^2 |V_{j-1,j}|^2 Q_{j-1} \tag{72}$$

and

$$\bar{Q}_{N-1} = \bar{Q}_{N-2} = 1 ,$$
$$\bar{Q}_{j-1} = \bar{Q}_j + \pi^2 |V_{j,j+1}|^2 \bar{Q}_{j+1} . \tag{73}$$

In Eqs. (67)–(73) both the intracontinuum couplings terms $V_{jj'} = V_{j\epsilon,j'\epsilon}$ and the intercontinuum couplings $V_{sn} \equiv V_{s,n\epsilon}$ are evaluated on the energy shell and therefore the label ϵ was omitted.

VI. ROTATIONAL STATES AND ENERGY PARTITIONING

In the last section, V, we presented a global model for a strictly collinear photofragmentation process. Mele and Okabe[1] investigated the vibrational excitation of CN radicals following the photodissociation of ICN, BrCN, ClCN, and HCN which, except for HCN, are quasilinear molecules in the (predissociation bound) excited states, and they found high rotational excitation of the CN radical. This does not contradict the linear hypothesis since, as Simons and Tasker pointed out,[8] a deviation from linearity $\lesssim 5°$ could give this high rotational excitation. However, if there is rotational excitation, the collinear results have to be modified in order to take into account the different number of rotational states available in each vibrational channel.[24]

Denoting by $P_n^c(E)$ the collinear probability for being at time $t = +\infty$ in the vibrational state n of CN at total energy E, then an approximate procedure[25,26] to include rotational states is the following: let $P(J/E)$ be the conditional probability for obtaining CN in the rotational level J. In the rigid-rotor harmonic oscillator (RRHO) approximation the rotational energy is given by

$$E_R^J = hcB_e J(J+1) , \tag{74}$$

while in the vibrating rotor (VR) level scheme

$$E_R^J = hcB_v J(J+1) , \tag{75}$$

where

$$B_v = B_e - \alpha_e(v + 1/2) . \tag{76}$$

Now, since part of the energy is in the rotational degrees of freedom, the vibrational + kinetic energy will be $E - E_R^J$ instead of E. Thus, $P(J/E)P_n^c(E - E_R^J)$ will be the probability of having the CN radical in the vibrational state n and rotational level J. The final (approximate) total probability for being in channel n is

$$P(n/E) = \sum_{J=0}^{J_n^*} P(J/E) P_n^c(E - E_R^J) , \tag{77}$$

where J_n^* is the maximum J compatible with energy conservation, i.e., for the VR level scheme,

$$hcB_n J_n^*(J_n^* + 1) = E - \hbar\omega_{BC}^{(d)}(n + 1/2) . \tag{78}$$

The total number of rotational states satisfying energy conservation is

$$N = \sum_{J=0}^{J_0^*} (2J+1) = J_0^*(J_0^* + 2) . \tag{79}$$

If we assume a Poisson distribution of the rotational levels

$$P(J/E) = \frac{\lambda^J}{J!} e^{-\lambda} \qquad J < J^* , \tag{80}$$

and if $J^* \gg 1$, we can transform the sum by an integral and $N \sim J_0^*(J_0^* + 1)$. Thus, finally,

$$P(n/E) = \frac{\int_0^{E-E_n} dE_R P_n^c(E - E_R) P(J/E_R)}{\int_0^{E-E_n} P(J/E_R)} , \tag{81}$$

with $E_n = \hbar\omega_{BC}^{(d)}(n + 1/2)$. A reasonable choice of the distribution parameter λ can rest on the available experimental data[1] identifying λ with the most probable rotational state of the diatomic photofragment.

TABLE I. Spectroscopic parameters used in the calculation.

HCN	ICN	CN ($B^2\Sigma^+$)
$k_{CH}^{(s)} = 5.8 \times 10^5$ dyn/cm	$k_{CI}^{(s)} = 3 \times 10^5$ dyn/cm	$\omega_{CN}^{(d)} = 2164.1$ cm^{-1}
$k_{CN}^{(s)} = 17.9 \times 10^5$ dyn/cm	$k_{CN}^{(s)} = 16.7 \times 10^5$ dyn/cm	$\bar{R}_{CN}^{(d)} = 1.15$ Å
$R_{CH}^{(s)} = 1.06$ Å	$R_{CI}^{(s)} = 2.12$ Å	
$R_{CN}^{(s)} = 1.156, 1.334$ Å	$R_{CN}^{(s)} = 1.159, 1.169, 1.183$ Å	
$\omega_1 = 2089$ cm^{-1}	$\omega_1 = 470$ cm^{-1}	
$\omega_2 = 3312$ cm^{-1}	$\omega_2 = 2158$ cm^{-1}	

VII. MODEL CALCULATIONS FOR THE PHOTOFRAGMENTATION OF SOME LINEAR XCN MOLECULES

We have presented explicit analytical results for the distribution of products and for the photofragmentation probabilities in direct photodissociation and predissociation of triatomics, which incorporate the effects of both interstate intrafragment coupling and intrastate, interfragment, continuum–continuum interactions. In what follows, we shall attempt to account for some features of a photofragmentation of the popular XCN molecules.[1] The following information is required for the application of our theory to a real photofragmentation process:

(1) Specification of the vibrational state (vv') of the "initial" $|s\rangle$ state. In the case of direct photodissociation at moderate (i.e., room) temperature, one can safely take $v = v' = 0$. In the case of predissociation, v and v' depend on the nature of the metastable bound state which is accessible by optical excitation. From a cursory examination of the available absorption spectra, it can be concluded that all the available[1] photofragmentation experiments on ICN, BrCN, and possibly HCN in the range 7.2–10.6 eV result in predissociation from Rydberg states.

(2) Information concerning molecular geometry in the bound state of the triatomic. The predissociating states of the halogen XCN (X = Cl, Br, I) molecules are linear,[10] so our model is strictly applicable. On the other hand, the low excited states of HCN are bent.[10b,11] Nevertheless, we shall also provide model calculations for this system.

(3) Interstate coupling terms, Eq. (39). These are determined by (a) the initial state quantum numbers (v, v') (Sec. A above), (b) the masses m_A, m_B, and m_C, (c) the equilibrium separations $\bar{R}_{AB}^{(s)}, \bar{R}_{BC}^{(s)}$ in the $|s\rangle$ state and $\bar{R}_{BC}^{(d)}$ in the dissociative state $|d\rangle$, (d) the molecular frequencies ω_1 and ω_2 in the $|s\rangle$ state and $\omega_{BC}^{(d)}$ of the diatomic fragment, (e) the reduced excess energy $E = (E_p - E_t)/\omega_{BC}^{(d)}$, where E_p is the photon energy while E_t corresponds to the dissociation threshold; E corresponds to the number of open vibrational channels; (f) the repulsive potential parameters A and α.

(4) The intercontinuum coupling terms, Eq. (41). These are determined by (a) the reduced mass m, Eq. (46), (b) the excess reduced energy E, and (c) the exponent α of the repulsive potential.

We have noted in Point (1) above that the majority of the available data for photofragmentation of XCN molecules involves predissociation[7] and, unfortunately, the identity of the (vv') nuclear state from which predissociation occurs is not known. Therefore, it is impossible at present to provide a quantitative account in terms of our model for the experimental data of Mele and Okabe.[1] Furthermore, calculation of the multidimensional Franck–Condon factors [Point (3)] is fraught with difficulties as the spectroscopic constants for the predissociating $|s\rangle$ states are unknown. We have therefore performed a set of model calculations for ICN and HCN in an attempt to elucidate the gross features of the photofragmentation of linear triatomics. The input data were as follows: (i) We have chosen $(v, v') = (0, 0)$, $(0, 1)$, and $(1, 0)$; (ii) The spectroscopic constants for the $|s\rangle$ state were taken as those corresponding to the ground state (Table I); (iii) The spectroscopic data for the CN radical were taken as those for CN($B^2\Sigma$); (iv) the reduced energy E was calculated (Table II) for the experimental excitation energies of Mele and Okabe[1]; and (v) the repulsive parameter α was roughly estimated from the relation

$$\alpha = L^{-1} \frac{m_C}{m_B + m_C} \left(\frac{\hbar}{\mu_{BC}^{1/2} k_{BC}^{1/2}} \right)^{1/2}, \tag{82}$$

where L is the range of the repulsive potential. For ICN, Holdy *et al.*[5] give $L \cong 0.15$ Å and $\alpha \simeq 0.17$. A reasonable universal estimate $L = 0.2$ Å for a variety of systems was provided[21] resulting in $\alpha \simeq 0.13$ for XCN molecules. The repulsive parameter was thus varied in the range $\alpha = 0.1$–0.2; (vi) the pre-exponential term A, of the repulsive potential. For ICN, Holdy *et al.* give $A = 0.9 \times 10^7$, while for HCN Band and Freed[9] have

TABLE II. Experimental data for photofragmentation of HCN and ICN.[1]

Molecule	Excitation energy $\langle E_e \rangle$ (eV)	Nature of photofragmentation	Average excess energy $\langle \Delta E7 \rangle = \langle E_e \rangle - E_t$ (eV)	Rotational distribution parameter λ
HCN	Br lamp 8.4		(0.17)	6
	Xe lamp 8.4, 9.5		1.31	18
	Kr lamp 10, 10.6		1.98	23
ICN	Hg lamp 6.7	Photodissociation	0.39	6
	Br lamp 7.2–8.5	Predissociation	1.43	23
	Xe lamp 8.4, 9.5	Predissociation	2.1	40
	Kr lamp 10, 10.6	Predissociation	3.9	40

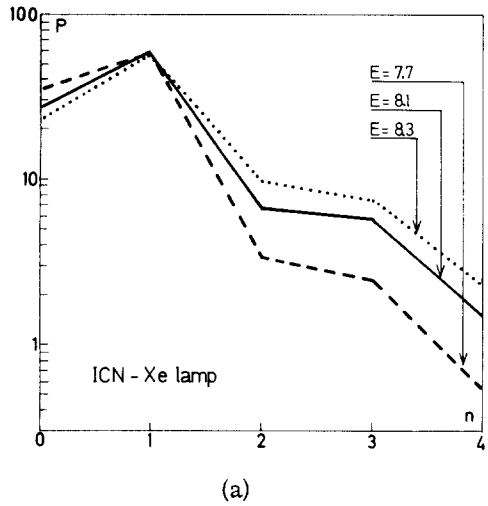

(a)

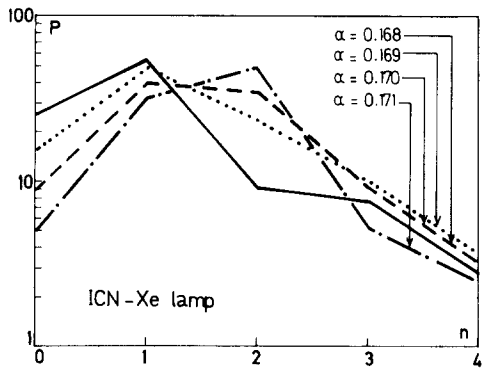

(b)

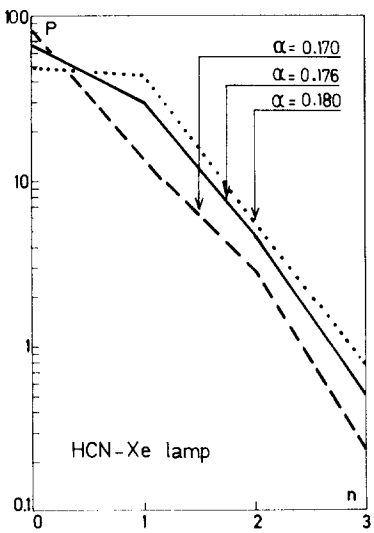

(c)

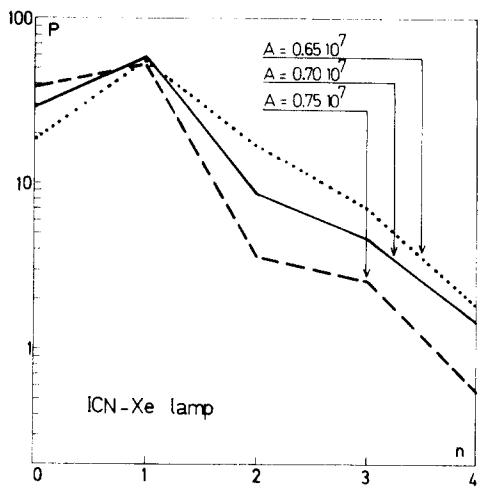

(d)

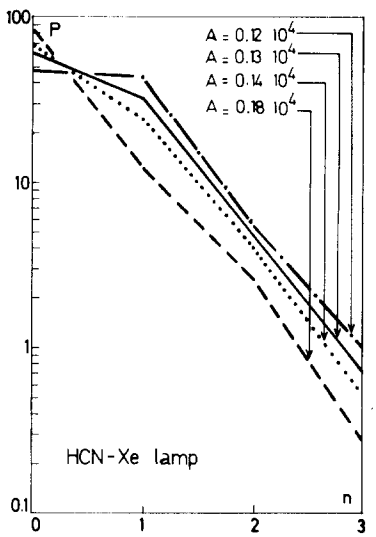

(e)

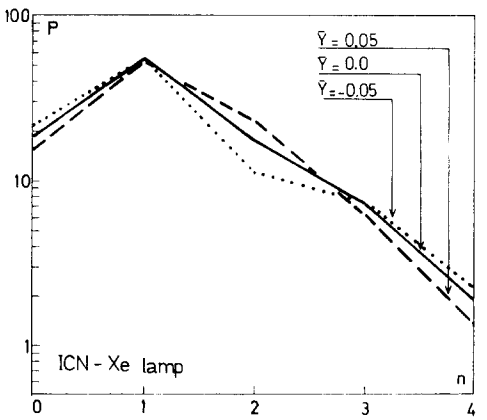

(f)

FIG. 1. (a) Vibrational population of CN from ICN irradiated by the Xe lamp, in relative coordinate basis, for $\alpha = 0.1766$ ($L = 0.15$ Å), $A = 0.65 \times 10^9$ (0.174×10^7 eV), $\lambda = 40$, $\bar{y} = 0.07$ (0.34×10^{-4} Å). Total population is arbitrarily taken as 100. (b) Same parameters as in Fig. 1(a) for distorted wave basis, except $E = 8.3$ (2.22 eV), $A = 0.35 \times 10^7$ (0.94×10^6 eV), $\lambda = 0$, $\bar{y} = 0$. (c) Vibrational population of CN for HCN irradiated by the Xe lamp, in distorted wave basis, for $E = 5.2$ (1.4 eV), $A = 0.13 \times 10^4$ (0.358×10^3 eV), $\lambda = 0$, $\bar{y} = 0$. Total population is taken as 100. (d) Same as in Fig. 1(a), with $E = 8.3$ (2.22 eV) and $\bar{y} = 0$. (e) Same as in Fig. 1(c), with $E = 5.4$ (1.45 eV) and $\alpha = 0.1766$ ($L = 0.15$ Å). (f) Same as in Fig. 1(a), with $E = 8.4$ (2.22 eV).

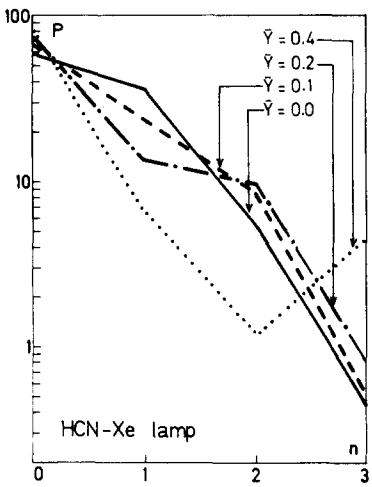

(g)

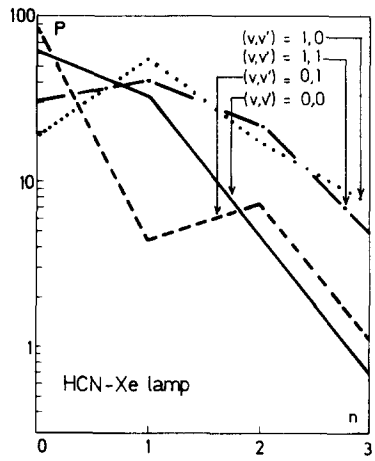

(h)

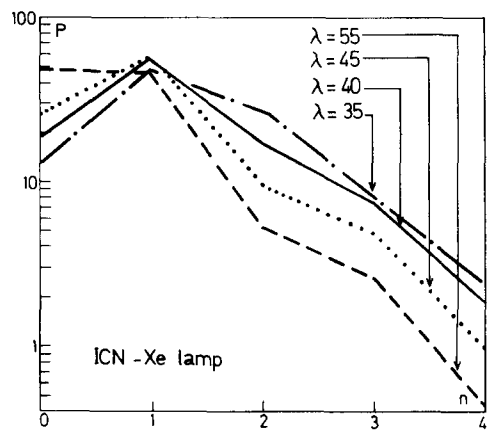

(i)

FIG. 1. *Cont'd.* (g) Same as in Fig. 1(c), with $E = 5.0$ (1.34 eV) and $\alpha = 0.1766$ ($L = 0.15$ Å), $A = 0.12 \times 10^4$ (0.32×10^3 eV). (h) Same as in Fig. 1(c), with $E = 5.4$ (1.45 eV) and $\alpha = 0.1766$ ($L = 0.15$Å). (i) Same as in Fig. 1(a), with $E = 8.3$ (2.22 eV).

chosen $A = 3.6 \times 10^5$. Again, this parameter was varied in a reasonable range $A = 0.5 \times 10^7 - 10^7$ for ICN and over a wide region for HCN; (vii) the parameter λ, introduced in Eq. (80), which specifies the rotational distribution. "Best choice" of this parameter from the available experimental data[1] is given in Table II. Numerical calculations were performed using both the relative coordinate representation (Sec. II) and the first-order distorted wave basis (Sec. IV).

A. Model calculations of vibrational distribution

We have conducted a series of model calculations to assess the dependence of the vibrational distribution on the excess energy, on the various molecular parameters, and on the final rotational distribution. The spectroscopic molecular data, i.e., atomic masses and frequencies, are those appropriate for ICN and HCN (Table I). These calculations were performed using the global model advanced herein and were conducted utilizing (1) the relative coordinate representation (RC), and (2) the first-order distorted wave approximation (FODWA). From these results, summarized in Figs. 1(a)–1(j), we conclude the following:

(a) The vibrational distribution is broader with increasing the excess energy E [Fig. 1(a)];

(b) The vibrational distribution is very sensitive to the parameters A and α characterizing the repulsive potential, as is evident from Figs. 1(b)–1(e). Increasing the range of the potential, i.e., decreasing α, which affects both intrafragment and interfragment coupling, results in an enhanced population of the lower n states and a sharper vibrational distribution. Increasing the pre-exponential potential parameter A, which affects only intrafragment coupling, has a similar effect as decreasing α.

(c) The configurational change $\bar{y}$ of the B–C bond (which affects the intrafragment coupling) modifies the distribution [Figs. 1(f) and 1(g)], depending not only on the magnitude but also on the sign of $\bar{y}$. For high values of $\bar{y}$ the distribution is not monotonic [Fig. 1(g)]. However, such appreciable configurational changes are not encountered in real life (see Table I);

(d) The vibrational population (vv') of the initial state $|s\rangle$ drastically modifies the vibrational distribution [Fig. 1(h)]. While $v = v' = 0$ usually results in a monotonously decreasing distribution with increasing n, for other (vv') values P_n peaks around $n > 1$. The latter case may be appropriate for predissociation;

(e) The effects of final distribution of rotational states, expressed in terms of the parameter λ, Eq. (80), are presented in Fig. 1(i). Increasing the rotational energy of the diatomic fragment is roughly equivalent to the decrease of the excess energy E, as expected.

Finally, in Fig. 2, we compare the results obtained using the RC representation and the FODWA for HCN at $E = 7.0$ (appropriate for excitation by the Kr lamp), together with the available experimental data. Good agreement between the results of the two methods is obtained, as is expected from the fact that in this case

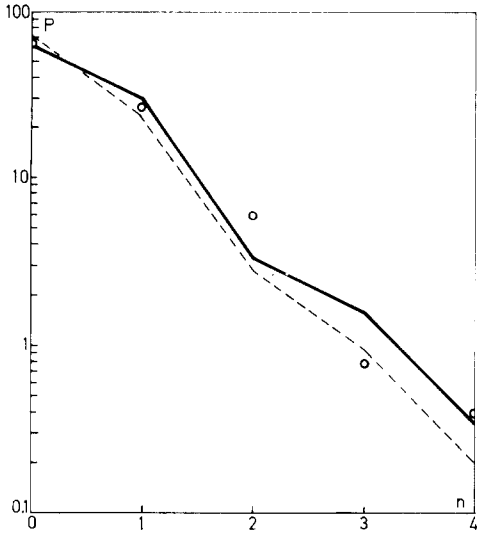

FIG. 2. Vibrational population of CN from HCN irradiated by the Kr lamp in distorted wave (—) and relative coordinate bases (---), for $E=7.0$ (1.88 eV), $\alpha=0.1766$ ($L=0.15$ Å), $A=0.16\times10^4$(0.43×10^3 eV), $\lambda=0$, $\bar{y}=0$. The points represent the experimental data of Ref. 1.

$m \ll 1$ and thus $\bar{m} \sim m$. The case for ICN is different ($m \sim 1$), and we have observed large discrepancies between the results obtained by the two approaches. A similar discrepancy was found in energy transfer problems where the RC representation was very superior compared to FODWA.[16,17] In the present case, in the absence of comparison with full quantum mechanical results for the same model, no assessments concerning

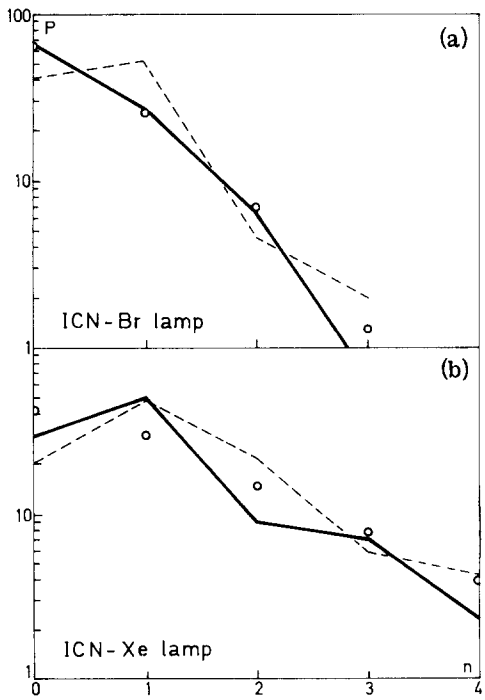

FIG. 3. Vibrational population of CN from ICN irradiated by the Br lamp, $E=5.8$ (1.55 eV) (a), and by the Xe lamp, $E=8.6$ (2.30 eV) (b) in relative coordinates basis, for $\alpha=0.175$, $A=0.65\times10^7$ (0.17×10^7 eV), $\lambda=25$, $\bar{y}=-0.07$ (-0.34×10^{-4} Å). With (—) and without (---) interstate couplings.

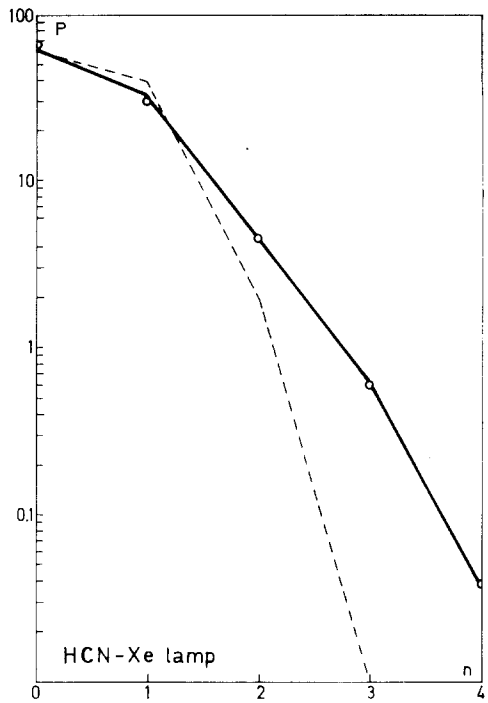

FIG. 4. Vibrational population of CN from HCN irradiated by the Xe lamp, in distorted wave basis, for $E=5.4$ (1.45 eV), $\alpha=0.1766$ ($L=0.15$ Å), $A=0.13\times10^4$ (0.35×10^3 eV), $\lambda=0$, $\bar{y}=0$, with (—) and without (---) interstate couplings.

the RC representation can be made. It should be kept in mind that this representation is affecting both the intra- and interfragment couplings.

B. The effects of intercontinuum coupling

There has been a lively controversy[7,8,9,12b] as to whether the major factor affecting the vibrational distribution involves interfragment (continuum–continuum) or intrafragment (bound–continuum) Franck–Condon-type coupling. To resolve this point we have conducted a series of calculations using the global model which incorporates both effects, and compared these data with the results of other calculations where the effects of intercontinuum coupling are neglected, by setting $F(n,n')=\delta_{nn'}$ in Eq. (67). As evident from Figs. 3–5, the effects of continuum–continuum coupling are by no means negligible. For ICN at $E=5.8$, $E=8.6$, and $E=14.7$ eV, the intercontinuum coupling increases P_n at $n=0$ by about 30%, while at high n values P_n is decreased by a numerical n factor of ~2–3. For HCN at $E=5.4$ and $E=8$, intercontinuum coupling effects are not dramatic at low $n=0.1$; however, at higher n values P is increased by a numerical factor 5–10. Thus, intercontinuum couplings drastically modify the population of high vibrational levels. Thus we do not concur with the qualitative conclusion of Band and Freed[9] that continuum–continuum interactions are negligible, and we assert that these effects have to be incorporated in any quantitative theory of photofragmentation.

C. Some naive fits of experimental data

We have attempted to account for the experimental vibrational distribution (Table I) observed in the pre-

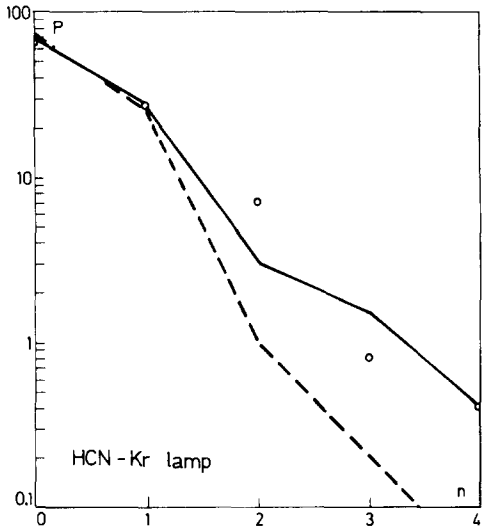

FIG. 5. Vibrational population of CN from HCN irradiated by the Kr lamp in distorted wave basis for $E=8.0$ (2.14 eV), $\alpha=0.1766$ ($L=0.15$ Å), $A=0.18\times10^4$ (0.48×10^3 eV), $\lambda=0$, $\bar{y}=0$, with (——) and without (---) interstate coupling.

dissociation of ICN at $E=5.8$, 8.4, and 14.7 eV and of HCN at $E=5.4$ and 8.0 eV by assuming photofragmentation from the initial $|s,0,0\rangle$ state, an assumption which cannot be taken seriously. Nevertheless, we have chosen the optimal repulsive potential parameters A and α together with the reasonable value $|\bar{y}| \simeq 0$–0.1 and a value of λ close to experimental values according to Table I (but this latter parameter does not appreciably affect the results). The results of our calculation for ICN and HCN over the available energy range[1] are presented in Figs. 6–8. The "best" potential parameters (which are independent of E) are summarized in Table III. For ICN the potential parameters are in reasonable agreement with those of Holdy *et al.*[5] For HCN, a marked difference between our pre-exponential term A and that used by Band and Freed is observed. We believe that this discrepancy cannot be resolved at present on the basis of the available experimental P_n data.

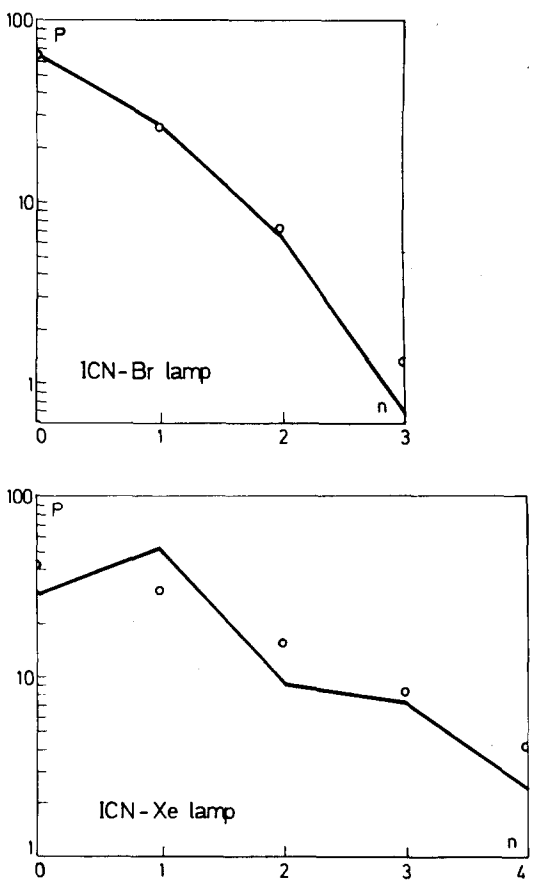

FIG. 6. Vibrational population of CN from ICN irradiated by the Br lamp, $E=5.8$ (1.55 eV) (a) and by the Xe lamp, $E=8.6$ (2.30 eV) (b) in relative coordinates basis, for $\alpha=0.1766$ ($L=0.15$ Å), $A=0.65\times10^7$ (0.17×10^7), $\lambda=25$, $\bar{y}=-0.07$ (-0.34×10^{-4} Å).

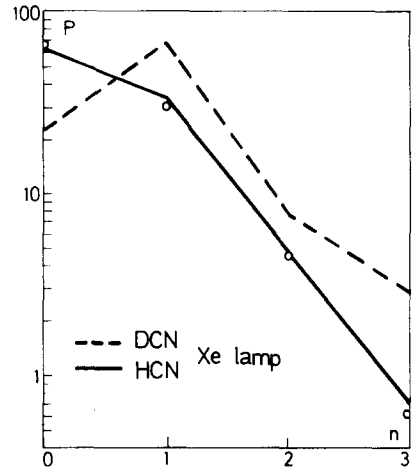

FIG. 7. Vibrational population of CN for HCN (——) and DCN (---) irradiated by the Xe lamp in distorted wave basis for $E=5.4$ (1.45 eV), $\alpha=0.1766$ ($L=0.15$ Å), $A=0.13\times10^4$ (0.35×10^3 eV), $\lambda=0$, $\bar{y}=0$.

D. Isotope effects

We now proceed to discuss two types of isotope effects in the photofragmentation of triatomics: (a) the

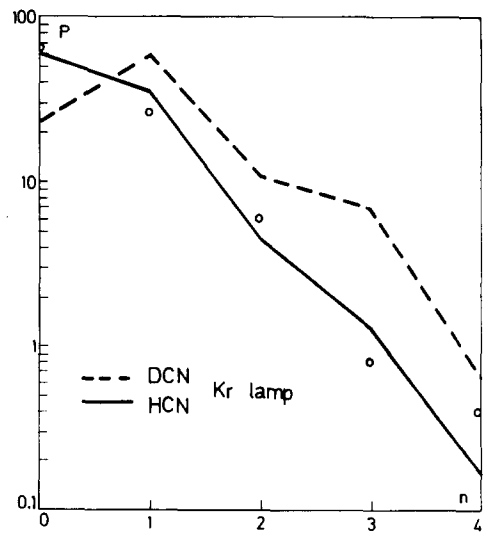

FIG. 8. Vibrational population of CN for HCN (——) and DCN (---) irradiated by the Kr lamp in distorted wave basis for $E=8.0$ (2.15 eV), $\alpha=0.1766$ ($L=0.15$ Å), $A=0.13\times10^4$ (0.35×10^3 eV), $\lambda=50$, $\bar{y}=0$.

TABLE III. Repulsive potential parameters.

Molecule		A	α
HCN	a	3.62×10^5	0.1760
	b	1.3×10^3	0.1766
ICN	a	3.16×10^7	0.0876
	b	0.65×10^7 [d]	0.1766
		$[0.27\times10^7]$ [e]	
	c	0.91×10^7	0.1760

[a]Reference 9.
[b]Present work.
[c]Reference 5.
[d]Relative coordinates.
[e]Distorted waves.

vibrational distribution, Eq. (67), and (b) the relative photofragmentation probabilities, Eq. (69). We shall address ourselves to the HCN molecule, comparing our results with the recent interesting work of Band and Freed.[9]

In view of the reasonable fit of the HCN data (Figs. 7 and 8) with our global model using physically acceptable values of the potential parameters, we can provide an estimate of the deuterium isotope effect on the vibrational distribution. Using the same value of α for DCN as for HCN, we now predict the vibrational distribution in DCN for the excess energies $E=5.4$ and $E=8$. This prediction is shown in Figs. 7 and 8, and we expect the vibrational distribution in the photofragmentation of DCN to be characterized by a lower value of P_0 and by somewhat higher values of P_1–P_3 than HCN. The isotope effect on P_n is quite appreciable, $P_0(\mathrm{DCN})/P_0(\mathrm{HCN}) \simeq 0.3$ and $P_3(\mathrm{DCN})/P_3(\mathrm{HCN}) \simeq 5$, at both energies so that "ordinary" and "inverse" isotope effects are exhibited for different n values. There are some quantitative differences between our prediction and that given by Band and Freed,[9] who predict that $P_0(\mathrm{HCN})/P_0(\mathrm{DCN}) \simeq 1$ and $P_3(\mathrm{DCN})/P_3(\mathrm{HCN}) \simeq 3$; however, this is not serious in view of the rather different (unreliable) potential parameters used in both calculations. Obviously, studies of the isotope effects of P_n will be useful and informative.

Band and Freed[9] have recently argued that the direct photodissociation of DCN will not be observable as the isotope effect on the absorption cross section is $\gamma_s(\mathrm{DCN})/\gamma_s(\mathrm{HCN}) \sim 10^{-14}$. It should be noted that this astronomical isotope effect also applies for predissociation from the $(v=0,\ v'=0)$ state if this is the dominating photofragmentation mechanism in the energy range studied by us. The theoretical prediction of Band and Freed[9] contradicts both physical intuition and experience. We have conducted a series of numerical model calculations of the photofragmentation probability γ_s, Eq. (69), of HCN and DCN at $E=5$. In view of our ignorance of the potential parameter A, it was varied over a broad range (Table IV). Taking our value $A=1.5\times10^3$ obtained from the fit of the P_n data (Sec. V.C) we predict $\gamma_s(\mathrm{DCN})/\gamma_s(\mathrm{HCN}) \simeq 0.25$, while Band and Freed's pre-exponential parameter $A=3.6\times10^5$ yields $\gamma_s(\mathrm{DCN})/\gamma_s(\mathrm{HCN}) \simeq 10^2$. Our prediction results in a reasonable isotope effect, as encountered in experimental studies of photofragmentation of three and four atom molecules.[13] We note that only for extremely large unphysical values of $A=10^6$–10^7 for HCN and DCN astronomical isotope effects $\gamma_s(\mathrm{DCN})/\gamma_s(\mathrm{HCN}) \simeq 10^{-6}$, which are somewhat lower than envisioned by Band and Freed,[9] are predicted. However, for such high A values the resulting photofragmentation probabilities are exceedingly low, $\gamma_s(\mathrm{HCN})=10^{-14}$–$10^{-22}$. To provide a rough idea regarding the expected order of the magnitude of γ_s for a physical system, let us consider the cross sections for direct photodissociation. The cross section σ at the wavelength λ can be expressed in the form

$$\sigma=\frac{8\pi^2}{3}\lambda^{-1}|\mu_{fi}|^2\,, \tag{83}$$

where μ_{fi} is the transition moment for bound–continuum transition. As the continuum states are energy normalized $|\mu_{fi}|^2$ is given in the units of e^2l^2/E. Making use of Eq. (69), we can identify γ_s with $|\mu_{fi}|^2$, getting

$$\sigma=\frac{8\pi^2}{3}\lambda^{-1}|\langle s|\mu|d\rangle|^2\gamma_s\,. \tag{84}$$

As an order of magnitude estimate we take $\lambda=1500$ Å, $\langle s|\mu|d\rangle \simeq 0.1$ D for the electronic transition moment, and $\sigma=10^{-18}$–10^{-19} cm^2 (which corresponds to an absorption coefficient of 10^2–$10^3\ M^{-1}\cdot\mathrm{cm}^{-1}$). We then get $\gamma_s \simeq 1.5\times10^{12}\,(\mathrm{erg})^{-1}$–$1.5\times10^{11}\,(\mathrm{erg})^{-1}$. In the dimensionless units of Table IV, we estimate $\gamma_s \simeq 0.6$–0.06. Thus high values of $A>2\times10^4$ will result in too low values of γ_s for the photodissociation of HCN. As only these high A values are associated with abnormally large isotope effect on γ_s, we may assert that only our choice of the A parameter for HCN (Table 9) is acceptable, as it yields (Table IV) to reasonable values of γ_s. We conclude that the cross sections for direct photodissociation (and the predissociation probabilities) of HCN and DCN in the energy range $E=5$–10 will exhibit a normal, ordinary isotope effect.

TABLE IV. Photodissociation cross sections for HCN and DCN.

$E=5$(1.34 eV)	$\alpha=0.1766$ ($L=0.149$ Å)	$\lambda=0$
$\bar{z}=40.1$ (1.06 Å)	$\bar{\gamma}=0.1$ (0.5 10^{-4} Å)	
$\Omega_{CN}=1.$	$\Omega_{HC}=1.5$	$\Omega_{DC}=1.1$
$m_{HCN}=0.0432$		$m_{DCN}=0.0832$

A(×0.268 eV)	γ_s(HCN)[a]	γ_s(DCN)
10^3	0.12×10^{-2}	0.39×10^{-3}
2×10^3	0.2	0.9×10^{-1}
3×10^3	0.67	0.587
4×10^3	0.95	0.104×10^{1}
5×10^3	0.99	0.116×10^{1}
10^4	0.38	0.34
2×10^4	0.38×10^{-1}	0.15×10^{-1}
4×10^4	0.12×10^{-2}	0.13×10^{-3}
10^5	0.29×10^{-5}	0.32×10^{-7}
10^6	0.14×10^{-14}	0.68×10^{-20}
10^7	0.46×10^{-22}	0.19×10^{-28}

[a]γ_s in the units of $1/\omega_{CN}^{(d)}$.

VIII. CONCLUDING REMARKS

We are able to incorporate all the physical characteristics of the vibrational energy partitioning in the linear photofragmentation problem. The main new features of the present work involve the detailed treatment of the intercontinuum intrafragment coupling as well as the role of rotational states. Two types of additional input information are still missing. First, spectroscopic data concerning the nature and the molecular constants of the predissociating states are needed. Second, reliable information regarding the parameters of the repulsive potential is required. An independent source of information concerning the latter problem for direct photodissociation may be obtained from the analysis of the experimental absorption line shape functions according to Eq. (69). This work is now in progress.

ACKNOWLEDGMENTS

One of us (J. A. Beswick) would like to acknowledge the benefit of helpful discussions with Dr. M. Baer and Professor M. Berry during the workshop on Molecular Collisions organized by C. Moser at C.E.C.A.M., Orsay, France, July–August 1975.

APPENDIX A: EVALUATION OF TWO-DIMENSIONAL FRANCK-CONDON FACTORS FOR RELATIVE COORDINATES

Using the generator form of the Hermite polynomials appearing in the harmonic oscillator wavefunctions,

$$H_n(q)=\left(\frac{\partial}{\partial t}\right)^n \exp(-t^2+2tq)\Big|_{t=0}\,, \tag{A1}$$

we have for Eq. (33)

$$\langle s,v,v'|d,n,\epsilon\rangle=(\det)^{1/2}\pi^{-3/4}2^{-(v+v'+n)/2}(v!\,v'!\,n!)^{-1/2}$$
$$\times\int_{-\infty}^{\infty}dz\,\phi_\epsilon(z)\int_{-\infty}^{\infty}dy\,e^{-(q_1^2+q_2^2+y^2)/2}\left(\frac{\partial}{\partial t_1}\right)^v\left(\frac{\partial}{\partial t_2}\right)^{v'}\left(\frac{\partial}{\partial t_3}\right)^n\exp[-(t_1^2+t_2^2+t_3^2)+2t_1q_1+2t_2q_2+2t_3y]\Big|_{t_1,t_2,t_3=0}\,. \tag{A2}$$

Integration over coordinate y can now be performed by writing q_1 and q_2 of y and z by means of the transformation Eq. (25). The result can be recast in the form

$$\langle s,v,v'|d,n,\epsilon\rangle=(\det)^{1/2}\pi^{-1/4}(1+C_{12}^2+C_{22}^2)^{-1/2}$$
$$\times 2^{-(v+v'+n-1)/2}(v!\,v'!\,n!)^{-1/2}\left(\frac{\partial}{\partial t_1}\right)^v\left(\frac{\partial}{\partial t_2}\right)^{v'}\left(\frac{\partial}{\partial t_3}\right)^n\exp[f(t_1,t_2,t_3)]\int_{\infty}^{\infty}dz\,\phi_\epsilon(z)\exp[-\tfrac{1}{2}\tilde{\omega}(z-\tilde{z})^2]\Big|_{t_1,t_2,t_3=0}\,, \tag{A3}$$

where

$$\tilde{\omega}=C_{11}^2+C_{21}^2-\frac{(C_{11}C_{12}+C_{21}C_{22})^2}{1+C_{12}^2+C_{22}^2}\,, \tag{A4}$$

$$\tilde{z}=\bar{z}+\tilde{\omega}^{-1}\left(\bar{y}\,\frac{C_{11}C_{12}+C_{21}C_{22}}{1+C_{12}^2+C_{22}^2}-(2t_1C_{12}+2t_2C_{22}+2t_3)\frac{(C_{11}C_{12}+C_{21}C_{22})}{1+C_{12}^2+C_{22}^2}+2t_1C_{11}+2t_2C_{21}\right) \tag{A5}$$

and

$$f(t_1,t_2,t_3)=\tfrac{1}{2}\tilde{\omega}(\tilde{z}-\bar{z})^2+\frac{1}{2(1+C_{12}^2+C_{22}^2)}\,[(C_{12}^2+C_{22}^2)\bar{y}+2t_1C_{12}+2t_2C_{22}+2t_3]^2-(2t_1C_{12}+2t_2C_{22})\bar{y}-\frac{(C_{12}^2+C_{22}^2)}{2}\bar{y}^2-(t_1^2+t_2^2+t_3^2)\,. \tag{A6}$$

Using now the well-known formula for the nth derivative of a product,

$$\frac{d^n}{dt^n}f(t)g(t)=\sum_{r=0}^{n}\binom{n}{r}\frac{d^rf}{dt^r}\frac{d^{n-r}g}{dt^{n-r}}\,. \tag{A7}$$

Equation (A3) results in Eq. (34).

APPENDIX B: FRANCK-CONDON FACTOR FOR DIRECT PHOTODISSOCIATION

When the initial bound state is characterized by $v=v'=0$, Eq. (34) yields

$$\langle s,0,0|d,n,\epsilon\rangle=(\det)^{1/2}\pi^{1/4}(8\bar{m}/\tilde{\omega}\beta\gamma 2^n n!)^{1/2}$$
$$\times\exp(A)\sum_{r=0}^{n}\binom{n}{r}d^{n-r}A_i^{(n-r)}(u)H_r(v)\,, \tag{B1}$$

with

$$A=\frac{\bar{y}^2}{2\beta}\left(1-\beta+\frac{\tau^2}{\beta\tilde{\omega}}\right)+\frac{\gamma^6}{12\tilde{\omega}^3}+\frac{\gamma^3}{2\tilde{\omega}}\left(z_t-\bar{z}-\frac{\tau\bar{y}}{\tilde{\omega}\beta}\right)\,,$$

$$\beta=1+C_{12}^2+C_{22}^2\,,\quad \tau=C_{11}C_{12}+C_{21}C_{22}\,,\quad \tilde{\omega}=C_{11}^2+C_{21}^2-\frac{\tau^2}{\beta}\,,$$

$$d=\frac{2\gamma\tau}{\tilde{\omega}\beta}\,,$$

$$u=\frac{\gamma^4}{4\tilde{\omega}^2}+\gamma\left(z_t-\bar{z}-\frac{\tau\bar{v}}{\tilde{\omega}\beta}\right),$$

$$v=\frac{\bar{v}}{\beta}\left(\beta-1-\frac{\tau^2}{\beta\tilde{\omega}}\right)+\frac{\gamma^3\tau}{2\tilde{\omega}^2\beta}, \tag{B2}$$

and

$$H_\tau(v)=\frac{d^\tau}{dt^\tau}(e^{-Bt^2+2tv})\Big|_{t=0}, \tag{B3}$$

with

$$B=1-\frac{2}{\beta}-\frac{2\tau^2}{\beta^2\tilde{\omega}}. \tag{B4}$$

[1]A. Mele and H. Okabe, J. Chem. Phys. **51**, 4798 (1969).

[2](a) G. E. Busch and K. R. Wilson, J. Chem. Phys. **56**, 3638 (1972). (b) J. H. Ling and K. R. Wilson, J. Chem. Phys. **63**, 101 (1975). (c) R. D. Clear, S. J. Riley, and K. R. Wilson, J. Chem. Phys. **63**, 1340 (1975). (d) R. J. Oldman, R. K. Sander, and K. R. Wilson, J. Chem. Phys. **63**, 4252 (1975).

[3]L. C. Lee and D. L. Judge, Can. J. Phys. **51**, 378 (1973).

[4](a) E. S. Yeug and C. Bradley-Moore, J. Am. Chem. Soc. **93**, 2059 (1971). (b) E. S. Yeug and C. Bradley-Moore, J. Chem. Phys. **58**, 3988 (1973).

[5]K. E. Holdy, L. C. Klotz, and K. R. Wilson, J. Chem. Phys. **52**, 4588 (1970).

[6]M. Shapiro and R. D. Levine, Chem. Phys. Lett. **5**, 499 (1970).

[7](a) S. Mukamel and J. Jortner, J. Chem. Phys. **60**, 4760 (1974); (b) S. Mukamel and J. Jortner, J. Chem. Phys. (to be published).

[8]J. P. Simons and P. W. Tasker, Mol. Phys. **26**, 1267 (1973); *ibid.* **27**, 1691 (1974).

[9](a) Y. B. Band and K. F. Freed, Chem. Phys. Lett. **28**, 328 (1974); (b) Y. B. Band and K. F. Freed, J. Chem. Phys. **63**, 3382 (1975); (c) *ibid.* **63**, 4479 (1975); (d) We were informed by Professor K. F. Freed that the calculations reported in Refs. 9(a) and 9(c) are incorrect, as they involved an algebraic error in the derivation of the C transformation matrix. We are grateful to Professor Freed and to Dr. Band for a discussion of this problem.

[10](a) G. W. King and A. W. Richardson, J. Mol. Spectrosc. **21**, 339, 353 (1966); (b) G. Herzberg and K. K. Innes, Can. J. of Phys. **35**, 842 (1957).

[11]G. Herzberg, *Electronic Spectra of Polyatomic Molecules*, (Van Nostrand, Toronto, 1966).

[12](a) C. E. Caplan and M. S. Child, Mol. Phys. **23**, 219 (1972); (b) M. J. Berry, Chem. Phys. Lett. **29**, 329 (1974).

[13](a) H. Abgrall and F. Fiquet-Fayard J. Chem. Phys. **60**, 11 (1974); (b) F. Fiquet-Fayard M. Sizun, and H. Abgrall, Chem. Phys. Lett. **37**, 72 (1976).

[14]D. Rapp and T. Kassal, Chem. Rev. **69**, 61 (1969).

[15]S. Mukamel, Ph.D. thesis, Tel-Aviv University, 1975.

[16]O. Atabek, J. A. Beswick, and R. Lefebvre, Chem. Phys. Lett. **32**, 28 (1975); *ibid.* **33**, 228 (1975).

[17]O. Atabek, J. A. Beswick, R. Lefebvre, S. Mukamel, and J. Jortner, Mol. Phys. **31**, 1 (1976).

[18]N. Rosen, J. Chem. Phys. **1**, 319 (1933).

[19]M. Abramowitz and I. A. Stegun, *Handbook of Mathematic Functions* (National Bureau of Standards, Washington, 1965).

[20]J. M. Jackson and N. F. Mott, Proc. R. Soc. London Ser. A **137**, 703 (1932).

[21]D. Secrest and B. R. Johnson, J. Chem. Phys. **45**, 4556 (1966).

[22]M. L. Goldberger and R. M. Watson, *Collision Theory* (Wiley, New York, 1964).

[23]L. Mower, Phys. Rev. **142**, 799 (1966).

[24]R. B. Bernstein and R. D. Levine, Chem. Phys. Lett. **29**, 314 (1974).

[25]M. Baer, J. Chem. Phys. **62**, 4545 (1975).

[26]J. L. Kinsey, J. Chem. Phys. **54**, 1206 (1971).